A Journal of the Gesellschaft Deutscher Chemiker

Angewandte International Edition GDCh Chemie

www.angewandte.org

Accepted Article

Title: Bridged Stilbenes: AIEgens Designed via a Simple Strategy to Control the Non-radiative Decay Pathway

Authors: Riki Iwai, Satoshi Suzuki, Shunsuke Sasaki, Amir Sharidan Sairi, Kazunobu Igawa, Tomoyoshi Suenobu, Keiji Morokuma, and Gen-ichi Konishi

To be cited as: *Angew. Chem. Int. Ed.* 10.1002/anie.202000943
Angew. Chem. 10.1002/ange.202000943

Link to VoR: http://dx.doi.org/10.1002/anie.202000943
http://dx.doi.org/10.1002/ange.202000943

WILEY-VCH

10.1002/anie.202000943

RESEARCH ARTICLE

WILEY-VCH

Bridged Stilbenes: AIEgens Designed via a Simple Strategy to Control the Non-radiative Decay Pathway

Riki Iwai,[a] Satoshi Suzuki*[b] Shunsuke Sasaki,[c] Amir Sharidan Sairi,[a] Kazunobu Igawa,[d] Tomoyoshi Suenobu,[e] Keiji Morokuma**[b] and Gen-ichi Konishi*[a]

Celebration for the 20th anniversary of aggregation-induced emission (AIE)

Abstract: To broaden the application of aggregation-induced emission (AIE) luminogens (AIEgens), the design of novel small-molecular dyes that exhibit high fluorescence quantum yield (Φ_{fl}) in the solid state is required. Considering that the mechanism of AIE can be rationalized based on steric avoidance of non-radiative decay pathways, a series of bridged stilbenes was designed, and their non-radiative decay pathways were investigated theoretically. Bridged stilbenes with short alkyl chains exhibited a strong fluorescence emission in solution and in the solid state, while bridged stilbenes with long alkyl chains exhibited AIE. Based on this theoretical prediction, we developed the bridged stilbenes **BPST[7]** and **DPB[7]**, which demonstrate excellent AIE behaviour.

Introduction

Over the last two decades, aggregation-induced emission (AIE)[1] has contributed to great developments in the fields of materials science,[2] analytical chemistry,[3] and life sciences.[4] In addition to conventional AIE-active compounds, such as derivatives of tetraarylsilole[5] and tetraphenylethene,[6] recent studies have found a wide variety of new AIE-active compounds. However, to further broaden the potential applications of AIE luminogens (AIEgens), the design of novel small-molecular dyes that also exhibit high fluorescence quantum yields (Φ_{fl}) in the solid state is required. The mechanism of AIE has been thoroughly investigated, which allows us to approach this task via rational molecular design. The characteristic phenomenon observed in AIEgens, i.e., quenching in solution and emitting light in the solid state, can be explained either by the 'restriction of intramolecular rotation' (RIR) model, the 'restriction of intramolecular motion' (RIM) model,[7] or by the 'restricted access to conical intersection' (RACI) model.[8]

In our previous studies, we discovered that bis(*N*,*N*-dialkylamino)anthracenes (**BDAAs**) display AIE.[9,10] We have reported that the mechanism of AIE for **BDAAs** can be explained as follows: 1) the ring-puckered conical intersection (CI) is lowered in energy via rotation of the amino group, which leads to internal conversion rather than emission in solution; 2) fast internal conversion in solution results in a low Φ_{fl} in solution; 3) given that ring puckering is prohibited in aggregated states, internal conversion is inhibited and therefore the Φ_{fl} in aggregated states is enhanced.[10] The term "aggregation-induced emission" refers to the induction of luminescence when aggregates form in solution. This definition does not include explanation of the non-radiative decay in solution. From the theoretical investigation of the photophysical processes of **BDAA** exhibiting AIE behavior in a single molecule,[10] we concluded that the essence of AIE should be explained by the "environment-responsive non-radiative decay" model, rather than an ambiguous phenomenology which involves obtaining luminescence by decreasing mobility in the aggregate state. Therefore, the rational design strategy for AIEgens from the viewpoint of theoretical chemistry is the control of conical intersection accessibility (CCIA).

The rational molecular design of AIEgens based on the RACI model or CCIA strategy has so far been limited to the design of dialkylaminoarene derivatives.[10,11] In the present study, we propose a paradigm shift in AIEgen design. Recent theoretical investigations have revealed that it is possible to analyze photophysical processes using a potential energy surface (PES) in the same manner as a classical thermal chemical reaction.[12] Controlling access to the CI enables the selective formation of fluorescent and non-fluorescent molecules, as if controlling access to the transition states determine reaction rate and selectivity of products. AIEgens that arise from the CCIA strategy should satisfy the following three conditions: 1) a CI that is low in energy whilst in solution in order to ensure that the AIEgen has a low Φ_{fl} in solution; 2) a non-radiative decay pathway that is inhibited by the surrounding molecules when the AIEgen is in the solid state or an aggregate. The AIEgen should also possess a molecular motion of large amplitude that gives rise to a non-radiative decay pathway; 3) the orbital overlap in the aggregate form should be low in order to avoid aggregation-caused quenching (ACQ). Thus, by identifying the non-radiative decay pathway of the AIEgen, one can understand how an AIEgen acquires a low Φ_{fl} in solution and a high Φ_{fl} in the aggregate form. Therefore, the rational design of AIEgens that arise from the CCIA strategy can be realized as follows: 1) search for π-conjugated systems as molecular core with known

[a] Prof. Dr. G. Konishi,* A. S. Sairi, R. Iwai
Department of Chemical Science and Engineering
Tokyo Institute of Technology
2-12-1-H-134 O-okayama, Meguro-ku, Tokyo 152-8552, Japan
E-mail: konishi.g.aa@m.titech.ac.jp
[b] Dr. S. Suzuki,* Prof. Dr. K. Morokuma
Fukui Institute for Fundamental Chemistry
Kyoto University
Takano-Nishibiraki-cho 34-4, Sakyou-ku, Kyoto 606-8103, Japan
E-mail: suzuki.satoshi.8v@kyoto-u.ac.jp
[c] Dr. S. Sasaki
Université de Nantes, CNRS
Institut des Matériaux Jean Rouxel, IMN
F-44000 Nantes, France
E-mail: shun.sasaki213@gmail.com
[d] Prof. Dr. K. Igawa
Institute for Materials Chemistry and Engineering
Kyushu University
Fukuoka 816-8580, Japan
[e] Prof. Dr. T. Suenobu
Department of Advanced Science and Biotechnology
Osaka University
Osaka University, 2-1 Yamada-oka, Suita, Osaka 565, Japan
[**] Prof. Keiji Morokuma was passed away at 27 Nov 2017.

non-radiative decay pathways; 2) structurally or electronically tune the system to lower the CI of the molecule; 3) design the molecular structure so that its non-radiative decay pathway has a molecular motion with large amplitude. In contrast, the molecular design of AIEgens using the RIR or RIM model aims to suppress the non-radiative decay pathway of the molecule in the solid state.[7] This is achieved via introduction of a large number of biaryl bonds or a bridged structure between neighboring aryl groups to a molecular core. The design strategy that we employ here attempts to determine the non-radiative decay pathway in advance, before we introduce bulky groups at a specific position so that this pathway is blocked in the solid state. Using this strategy, we can identify prospective AIEgens via theoretical calculations and subsequently develop simple high-performance AIEgens.

We chose a π-extended stilbene as the molecular skeleton, as the non-radiative decay pathway of stilbene[13] and that of tetraphenylethene (TPE) proceeds via flipping of the double bond.[14] Accordingly, we focused on this pathway and designed a molecule that is mechanically constrained around the stilbene double bond. This approach allowed us to control the energy level of the CI of the stilbene moiety. As reported previously,[15] by bridging one end of the C=C bond to one of the two phenyl rings, it is possible to create a structure similar to that of indene. The formation of this tightly twisted C=C structure is not energetically favorable and destabilizes the CI. The corresponding dye exhibits a high-energy CI, which renders the non-radiative decay less likely to occur. Consequently, the dye exhibits strong fluorescence in solution and in the solid state.[15] In this study, we demonstrate how a series of bridged stilbenes with different bridge lengths exhibit different photophysical properties. We show that quantum chemical calculations are able to predict that a loosely bridged C=C bond should have a low CI and thus almost no fluorescence in solution. Given that the twisted structure of the C=C bond should be suppressed in the solid state, loosely bridged stilbenes would also be expected to be AIEgens. We will show that the synthesized compounds show good agreement with the computational prediction. Furthermore, unlike stilbene, π-extended stilbenes exhibit fluorescence in the visible region, which would be attractive for applications in functional materials.

Results and Discussion

Initially, we investigated the photophysical properties of a series of stilbenes and bridged stilbenes. We calculated the photophysical properties, synthesized the compounds (**Figure 1**), experimentally measured their photophysical properties, and compared the experimental results with those of the theoretical calculations.

Theoretical Investigation of the Non-radiative Decay pathway for the Stilbenes and the Bridged Stilbenes

In the beginning, we determined the non-radiative decay pathway of stilbene (**ST**). It should be noted that a twisted-pyramidal conical intersection has been reported on the PES of stilbene.[13]

The minimum energy conical intersections (MECIs) of **ST** were calculated using spin-flip time-dependent density functional theory (TD-DFT) at the Becke-Half-and-Half LYP/6-31G+(d) level of theory using the branching-plane-updating method.[16] The Franck-Condon state (FC), the local minimum near the FC (S1min), and the intermediate near the CI (INT) were located using the same method. The transition state (TS) connecting S1min and INT was initially located at the TD-B3LYP/6-31+G(d) level of theory, but subsequently updated to the SFTD-BHHLYP/6-31G+(d) level of theory using TD-B3LYP Hessian matrix calculations. All calculations were performed using GAMESS (2019 Sep.) and Gaussian 16.C01.[17,18]

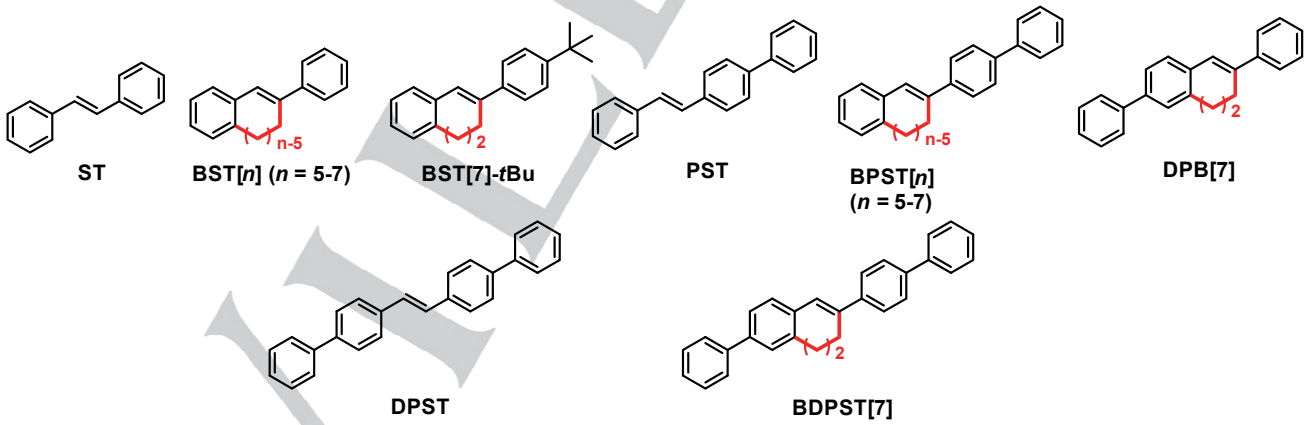

Figure 1. Structures of stilbenes and bridged-stilbenes.

We located the CI of **ST** and connected the most important points on the PES. As shown in **Figure 2(a)**, excited **ST** initially relaxes to a local minimum (S1min), where fluorescence occurs with an oscillator strength of ~0.6. After passing through a low barrier (7.88 kJ/mol), an intermediate structure INT is formed near to the CI. This structure has a small oscillator strength (~0.01), and thus this state can be thought of as a "dark state". After passing the INT, the S_1/S_0 MECI was found at 25.16 kJ/mol higher than the S1min. The structure of the MECI is a typical twisted-pyramidal structure (**Figure 3**). Note that this type of CI can lead E/Z isomerization. Because whether which isomer generates after passing through CI does not affect to the

fluorescence quantum yield, we do not show isomerization pathway in the figure.

To govern the photophysical properties of an AIEgen, the non-radiative decay pathway needs to be controlled. In the case of stilbene-based molecules, the simplest approach to achieve this is to mechanically restrict the twisting angle of the C=C bond. With this in mind, we considered a different series of compounds based around a bridged stilbene core (**BST[*n*]**). Here, *n* denotes the size of the *n*-membered ring used to restrict the movement of the C=C bond. Depending on the length of the alkyl chain, bridging phenyl groups gradually restrict the twisting angle of the C=C bond.

Subsequently, we calculated the non-radiative decay pathways for **BST[5]**, **BST[6]**, and **BST[7]**, and **Figure 2(b)** shows the energy diagram for the non-radiative decay process for each of these compounds. The FC for **BST[7]** is higher in energy than that of **BST[5]** and **BST[6]**, which can be rationalized in terms of the planarity of the π-conjugation observed in these molecules. In contrast to planar **BST[5]**, **BST[6]** and **BST[7]** exhibit a phenyl group that is shifted out of the plane (**Table 1**). This shift causes a decrease in planarity of the molecule, which reduces the effective conjugation length, especially in **BST[7]** (**Figure 4**), and thus causes a shorter absorption wavelength.

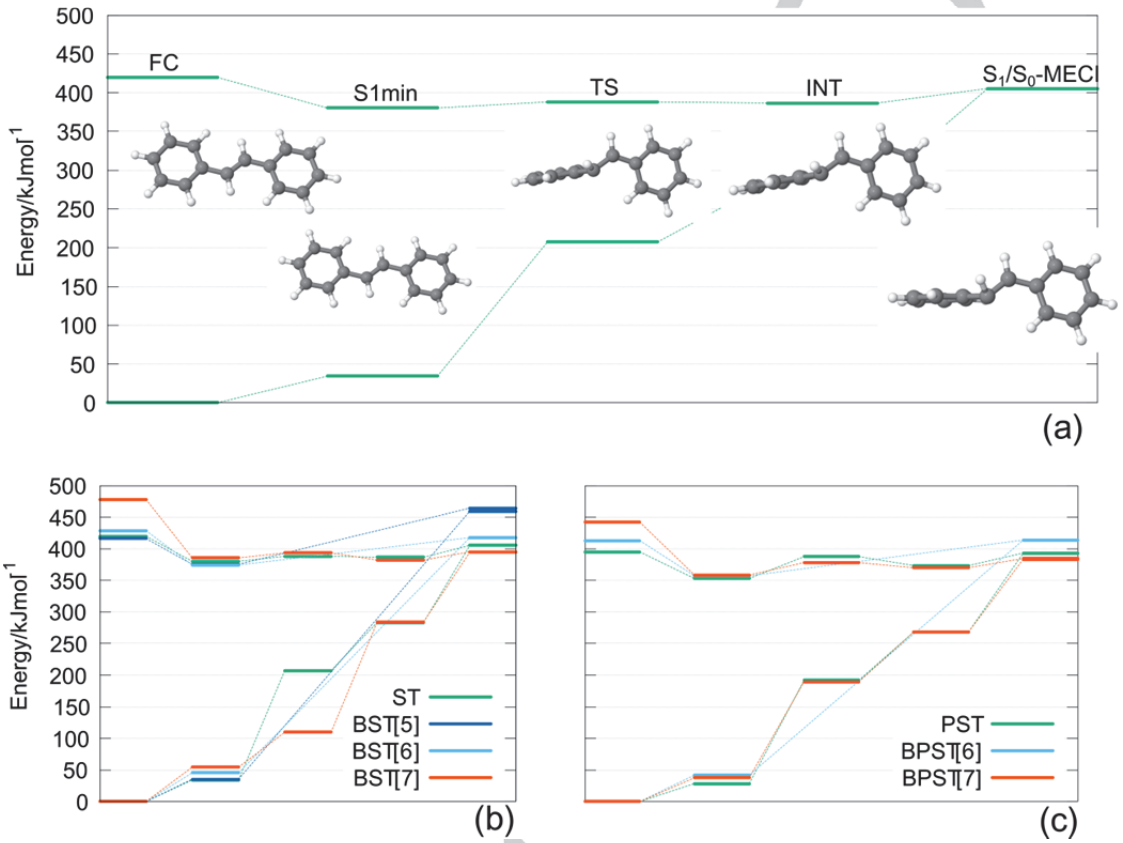

Figure 2. Energy diagram of (a) **ST** and **PST**, (b) bridged-stilbene **BST[*n*]**, and (c) bridged-phenylstilbene **BPST[*n*]**.

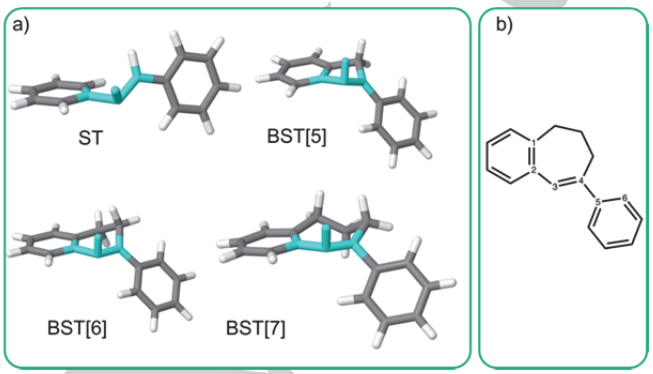

Figure 3 a) Structures of the CIs of **ST** and **BST[5-7]**. Twisted pyramidal structure of C=C double bonds are highlighted. b) Definition of atom-numbering for Table 1.

Table 1. Geometrical parameters of **BST[*n*].**[a]

Dihedral angle (degree)	**BST[7]**	**BST[6]**	**BST[5]**	Dihedral angle
1-2-3-4	-14.8	-14.6	0.0	1-2-3-4
2-3-4-5	0.9	2.7	0.0	2-3-4-5
3-4-5-6	218.4	149.7	180.0	3-4-5-6

[a]The atom-numbering scheme is shown in **Figure 3**.

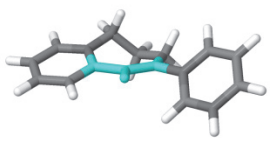

Figure 4 Structure of **BST[7]** in the FC state.

The energy of the MECIs descends in the order **BST[5]** > **BST[6]** > **BST[7]**. Although all these structures are similar, the shorter alkyl chain found in **BST[5]** is more rigid than those found in **BST[6]** and **BST[7]**, and thus raises the energy of the twisted-pyramidal CI (**Figure 3**). Conversely, the longer alkyl chains observed in **BST[6]** and **BST[7]** keep the energy of the CI low. A similar trend can be observed in the calculated Φ_{fl} in solution. The low barrier required to form the twisted-pyramidal MECI in **BST[7]** (9.59 kJ/mol) would suggest that **BST[7]** easily undergoes non-radiative decay, which would amount to a lowΦ_{fl} in solution. Conversely, the PES of **BST[6]** is different from that of **BST[7]**, i.e., the MECI for **BST[6]** resides at an energy level that is 43.26 kJ/mol higher than that of the S1min, which is still by 11.11 kJ/mol lower than the FC state. Thus, the non-radiative decay rate constant for BST[6] would be smaller than BST[7] and Φ_{fl} for BST[6] would be larger than BST[7]. The MECI of **BST[5]** is so high that it can be feasible expected that its non-radiative decay is very difficult to take place. In summary, it can be expected on the basis of the results of the theoretical calculations carried out in this study that the low MECI of **BST[7]** would render **BST[7]** a good prospective core structure for advanced AIEgens. **BST[7]** can be expected to have an accessible non-radiative decay pathway due to a large-amplitude molecular motion and therefore exhibit a low Φ_{fl} in solution.

As the calculated fluorescence wavelength of the **BST[*n*]** series is too short, we also considered bridged π-extended stilbenes (**BPST[*n*]**) to achieve emission at visible wavelengths. The calculated fluorescence wavelength of **BPST[7]** (370 nm) is within the visible region. The energy diagram for the **BPST[*n*]** series follows the same trend as that of the **BST[*n*]** series. Therefore, **BPST[7]** would be expected to be a good AIEgen candidate. A more detailed discussion of the energy diagrams is given later (*vide infra*).

Photophysical Properties of the Bridged Stilbenes

The structures and photophysical properties (absorption, fluorescence in solution and the solid state (polycrystalline solids), as well as Φ_{fl} values) of the synthesized stilbenes and bridged stilbenes are summarized in **Figures 1** and **S48** and **Table 2**. The synthetic methods used and all characterization data, including all spectra, are listed in the Supplementary Information. In some cases, the general synthetic route was not feasible. In the case of **BPST[7]**, when 4-biphenylboronic acid was used in the Suzuki-Miyaura cross-coupling reaction,[19] *p*-quarterphenyl, a compound that shows strong fluorescence in solution, was obtained as a byproduct. In order to avoid the formation of *p*-quarterphenyl, we performed a stepwise addition of the benzene rings.

We first examined a series of compounds that contains just two benzene rings, i.e., **ST** and **BST[*n*]**. While **ST** exhibits typical AIE behavior (Φ_{sol} = 0.01; Φ_{solid} = 0.62), **BST[5]** shows a strong fluorescence in the UV region in solution and in the solid state (Φ_{sol} = 0.40; Φ_{solid} = 0.79). **BST[6]**, which contains a more flexible alkyl chain, exhibits aggregation-induced emission enhancement (AIEE) behavior (Φ_{sol} = 0.06; Φ_{solid} = 0.26). While **BST[7]** is unfortunately a liquid at room temperature, **BST[7]-^{t}Bu** is a solid and shows AIE behavior. However, the fluorescence of the **BST** derivatives is in the UV region and, especially from an analytical and materials science perspective, fluorescence in the visible region is preferable. Therefore, we decided to examine bridged stilbenes with π-extended structures.

Subsequently, we examined a series of compounds that contain three benzene rings, 4-phenylstilbene (**PST**) and **BPST[*n*]**, and found that the extended π-conjugation observed in these molecules greatly affects their absorbance and fluorescence properties.

The shapes and vibrational structures of the absorption and fluorescence spectra of **BST[*n*]** are similar to previously reported spectra of **ST** [19] and the π-extended **ST**, poly(p-phenylene-vinylene).[20] **PST** and **BPST[*n*]** are related in a similar fashion. Accordingly, the lowest energy absorptions of **PST** and **BPST[*n*]** (***n* = 5-7**) can be assigned to the allowed ^{1}Ag → ^{1}Bu transition.[22]

Comparing the maximum absorption wavelengths (λ_{abs}) of **PST** and **BPST[*n*]** in solution, only **BPST[*n*]** exhibits a large hypsochromic shift. In contrast, the maximum fluorescence wavelengths (λ_{fl}) of **PST** and **BPST[*n*]** remain virtually unchanged. The large Stokes shifts (7200 cm^{-1}) observed for **BPST[7]** is in good agreement with the calculated results (**Figure 2b**). The FC state of **BPST[7]** is higher than that of **BPST[5]** and **BPST[6]**, albeit that the $S1_{min}$ state of all these compounds are similar. The structural change between the FC and $S1_{min}$ states of **BPST[7]** was confirmed by quantum calculations (**Figure S57**).

Diffuse-reflectance and fluorescence spectra of polycrystalline **PST** and **BPST[*n*]** are shown in **Figure S50**. Both the λ_{abs} and λ_{fl} values of polycrystalline **PST** and **BPST[*n*]** are bathochromically shifted relative to those in dilute solution. The same phenomenon has been reported for the prototypical AIEgen tetraphenylethene (TPE).[6] In the case of **BPST[*n*]**, intermolecular electronic interactions or conformational changes such as planarization-induced π-extension can be expected, which we will discuss during the x-ray crystallographic analysis (*vide infra*).

Unlike **ST**, **PST** exhibit strong fluorescence in the blue region of the visible spectrum in solution and the solid state (Φ_{sol} = 0.64; Φ_{solid} = 0.72), i.e., **PST** is unlike **ST** not an AIEgen. Similarly, **BPST[5]** and **BPST[6]** emit light in solution and the solid state. In contrast, **BPST[7]** shows perfect AIE behavior (Φ_{sol} = 0.01; Φ_{solid} = 0.95) with negligible emission in solution and high emission in the solid state. **DPB[7]**, which extends the π-conjugation of the system from a different position to **BPST[7]**, also shows excellent AIE properties (Φ_{sol} = 0.02; Φ_{solid} = 0.75). However, **BPST[8]** showed little fluorescence in solution or in the solid state (Φ_{sol} = 0.004; Φ_{solid} = 0.04). In regards to the absorption spectrum (λ_{max}), compared to **PST**, **BPST[5]** has increased planarity and shows longer π-conjugation length, **BPST[6]** has a similar degree of increased planarity, and both **BPST[7]** and **[8]** has decreased planarity and exhibits shorter π-conjugation length. The effect is reflected in the fluorescence spectra of these molecules (**Table 2**), i.e., λ_{abs} decreases with decreasing planarity of the molecule. **BPST[8]** exhibits not only the smallest λ_{abs}, but also the smallest absorption coefficient (ε), which is most likely due to a large twist around its C=C double bond. The shape of the fluorescence spectra of polycrystalline **BPST[8]** is similar to those of **BPST[*n*]** (***n* = 5-7**), albeit that the Φ_{fl} is very small (< 0.01). The reasons why **BPST[8]** does not exhibit fluorescence, neither in solution nor the solid, are that the

twisted structure is sufficiently large and that the conjugated system does not spread. In other words, this behavior can be explained by its twisted structure, which leads relatively smaller oscillator strength besides high accessibility toward MECI. Based on the results of the fluorescence spectra, it can be concluded that the flexible bridge provided by a 7-membered ring leads to the desired AIE effect in **PST**.

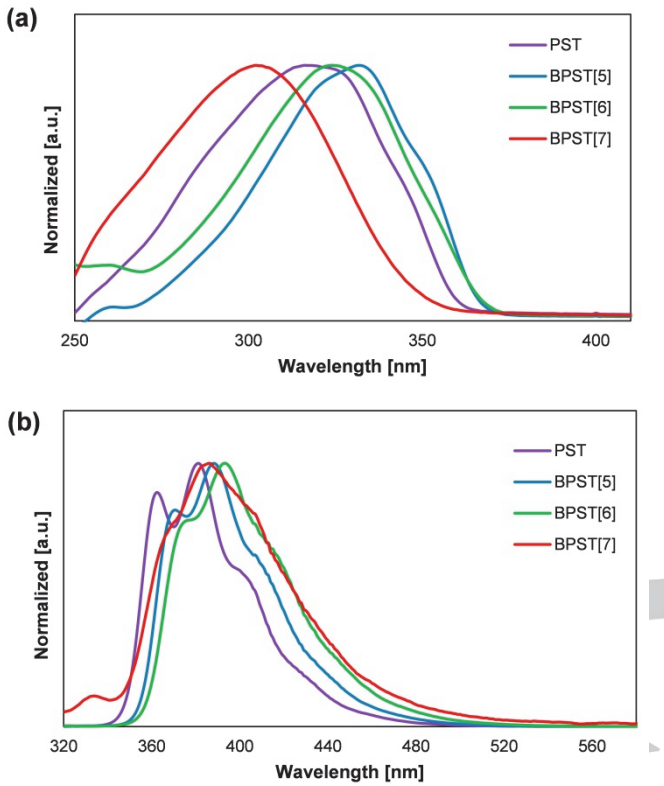

Figure 5. (a) UV absorption spectra of **PST**, **BPST[5]**, **BPST[6]**, and **BPST[7]** in THF (The concentration of each compound is 1.0×10^{-5} M). (b) Fluorescence spectra of **PST**, **BPST[5]**, **BPST[6]**, and **BPST[7]** in THF (The concentration of each compound is 1.0×10^{-5} M). Small peaks around 330 nm were assigned to Raman scattering.

We have also measured the fluorescence lifetime of **PST** and **BPST[*n*]** (*n* = 5-7) in THF and determined the non-radiative (k_{nr}) and radiative transition rates (k_r) (**Table S2**). The obtained k_{nr} of **PST** and **BPST[*n*]** (*n* = 5-7) are 3.3×10^8, 0.9×10^8, 1.4×10^8, and 3.7×10^9 [s^{-1}], respectively. The k_r of **PST** and **BPST[*n*]** (*n* = 5-7) are 8.0×10^8, 7.2×10^8, 6.6×10^8, and 4.8×10^7 [s^{-1}], respectively. Among these compounds, **BPST[7]** shows $k_r \ll k_{nr}$, while the other dyes exhibit $k_r \succ k_{nr}$. In other words, the reason that **BPST[7]** shows very weak fluorescence is due to its high k_{nr}. Comparing **PST**, **BPST[5]**, and **BPST[6]** with **BPST[7]** shows that the k_{nr} value of the latter is large albeit that the ε and k_r values are small. Therefore, the conformation of **BPST[7]** does not decrease the planarity and restrict the mode leading to MECI.

An aggregation experiment of **BPST[7]** was performed, albeit that the Φ_{fl} value was low (0.22). Furthermore, the fluorescence wavelength (λ_{max}) is shorter than that of the solid due to the shorter lengths of the aggregates of the conjugated system (**Table S1**).

4,4'-Diphenylstilbene (**DPST**) contains four benzene rings and shows strong fluorescence in solution, which is quenched by intermolecular interactions in the solid state (Φ_{sol} = 0.67; Φ_{solid} = 0.16). The fluorescence behavior of **DPST** is similar to that of poly(*p*-phenylene vinylene) (PPV).[23] In contrast, the bridged form of **DPST**, **BDPST[7]**, shows AIEE behavior (Φ_{sol} = 0.12; Φ_{solid} = 0.87), which suggests that the 7-membered ring structure contributes to the AIE effect, but does not compensate the effect of long conjugated systems such as PPV.

Table 2. Photophysical properties of the stilbenes and bridged stilbenes used in this study in solution and in the solid state.

Entry	Number of benzene rings	ε [M^{-1} cm^{-1}]	λ_{abs} [nm]	λ_{fl} (THF) [nm]	λ_{fl} (solid)[a] [nm]	Φ_{fl} (THF)	Φ_{fl} (solid)
ST	2	23000	297	350	382	0.01	0.62
BST[5]	2	25000	315	357	417	0.40	0.79
BST[6]	2	22000	306	365	399	0.06	0.26
BST[7]	2	22000	285	308	-[b]	0.001	-[b]
BST[7]-^{t}Bu	2	25000	288	360	380	0.01	0.11
PST	3	32000	317	381	434	0.71	0.72
BPST[5]	3	42000	332	388	434	0.89	0.62
BPST[6]	3	37000	324	393	445	0.83	0.82
BPST[7]	3	26000	304	386	418	0.01	0.95
BPST[8]	3	22000	288	341	405	0.004	< 0.01
DPB[7]	3	36000	309	385	413	0.02	0.75
DPST	4	49000	342	405	437	0.67	0.16
BDPST[7]	4	46000	321	408	431	0.12	0.87

[a] polycrystalline solids. [b] **BST[7]** is a liquid at room temperature.

The single-crystal x-ray structure of **BPST[7]** is shown in **Figure 6**. As the adjacent π-planes of molecules of **BPST[7]** do not adopt a face-to-face conformation, these do not resemble *H*-type aggregates. On the other hand, the excitation spectrum of **BPST[7]** in the crystal is red-shifted compared to the absorption spectrum of **BPST[7]** in solution (**Figure S48**). Considering the maximum wavelengths of absorption and fluorescence in solution and the polycrystalline solid, the effect of excitonic coupling or excimer formation could be one possible explanation for the observed phenomenon. The details of the photophysical process of polycrystalline **BPST[7]** will be investigated in the future.

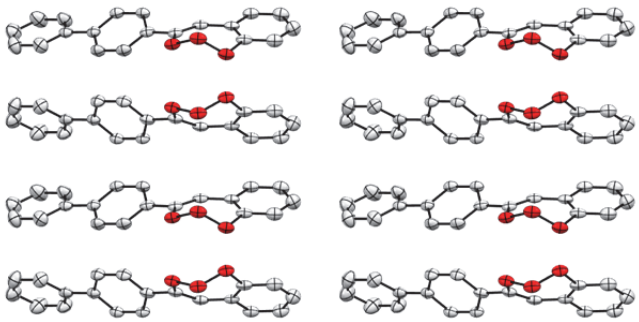

Crystal System	Monoclinic		
Space Group	*Pc*		
Cell Lengths (Å)	**a** 15.1833(14)	**b** 7.8455(5)	**c** 6.6878(4)
Cell Angles (°)	**α** 90	**β** 93.380(7)	**γ** 90
Cell Volume (Å^3)	795.27(10)		

Figure 6. ORTEP drawing of **BPST[7]** with thermal ellipsoids set at 60% probability. The carbons of bridged-alkyl chain are highlighted in red.

Both radiative and non-radiative decay processes can be observed in **BDPST[7]**. Picosecond laser-induced transient absorption measurements were carried out with a sub-nanosecond transient-absorption spectroscopy system based on the randomly interleaved pulse train (RIPT) method.[24] After photoirradiation, the S_1 state (S_1-S_n transient absorption: 720 nm) is generated, followed by fluorescence decay and the generation of an intermediate that follows the non-radiative decay pathway (420 nm) (**Figure S49**). The observed fluorescence lifetime was 0.17 ns. The lifetimes for the decay (0.21 ns) and the formation of the intermediate (0.24 ns) are approximately identical (**Figure S50**). Based on these results, it can be concluded that a structural change occurred due to internal conversion, as predicted by our calculations.

Fluorescence quantum yield of BST[n] and BPST[n]

In this section we will compare the experimental photophysical properties of the stilbenes and bridged stilbenes with their calculated values and respective PESs.

We first examined the **ST** and **BST[*n*]** series. The calculated order of the MECIs, **BST[5]** > **BST[6]** > **BST[7]**, successfully predicted the fluorescence Φ_{fl} observed in solution. Every member of the series **BST[*n*]** shows enhancement of the Φ_{fl} in the solid state. As shown in **Figure 3**, the twisted-pyramidal CI accompanies a large movement of the phenyl groups. Suppression of this large motion in the aggregate form causes AIE or AIEE.

Subsequently, we examined the **PST** and **BPST[*n*]** series. The calculated order of the MECIs, **BPST[5]** > **BPST[6]** > **BPST[7]**, corresponds to the order of the Φ_{fl} observed in solution. However, different from the **ST**/**BST[*n*]** series, **PST** and **BPST[6]** are emissive in solution. To understand the difference between the **ST**/**BST[*n*]** series and the **PST**/**BPST[*n*]** series, we compared the energy diagrams shown in **Figure 2**. Since the oscillator strengths do not differ much between these two series, it is the rate constant of the non-radiative decay process that mainly determines the Φ_{fl}. According to Engleman, the probability of non-radiative transition can be estimated using the height of the CI (= *E*(MECI) - *E*(S1min)) and the molecular nuclear relaxation energy (= *E*(FC) - *E*(S1min)).[25] Here, we employed a simpler parameter: ΔE = *E*(MECI) - *E*(FC). This value shows how accessible the MECI is. If ΔE is large, it means that the CI is inaccessible and that the non-radiative decay is unlikely to occur.

An extension of the π-conjugation of the system lowers the FC and the S1min. However, as shown in **Figure 2**, this has a relatively small effect on the TS and the MECI. At this point, we have not unambiguously determined the cause of this, but we currently think that this is partly due to the fact that the local distortion of the CI is not sensitive to distant substituent groups, while the orbitals in the FC are delocalized and therefore sensitive to distant substituent groups. In any case, the π-extension tends to increase ΔE and therefore raise the Φ_{fl}. Thus, the higher Φ_{fl} observed in **PST** relative to that in **ST** can be explained by the ΔE values that are given in **Table 3**. The high Φ_{fl} of **BPST[6]** can be explained in the same way as the ΔE for **BPST[6]** (+0.84 kJ/mol), which is higher than that of **BST[6]** (-11.11 kJ/mol).

The length of the alkyl chain affects both the FC and the MECI. Shorter alkyl chains keep the FC low and raise the MECI, which increases the Φ_{fl}. In contrast, longer alkyl chains raise the FC and keep the MECI low, which decreases the Φ_{fl}. Calculations were not performed for **BDPST[7]** and **DPST**, but can be interpreted in the same manner.

Table 3 ΔE values in kJ/mol for selected stilbenes and bridged stilbenes

ST	-14.41	**PST**	-2.01
BST[5]	+48.15	**BPST[5]**	Not calculated
BST[6]	-11.11	**BPST[6]**	+0.84
BST[7]	-82.82	**BPST[7]**	-57.69

Conclusion

We calculated the non-radiative decay pathway for stilbene (**ST**), which revealed that **ST** adopts a twisted-pyramidal structure at the conical intersection (CI). Based on the idea that control of conical intersection accessibility enables control of photophysical properties, we investigated a series of bridged stilbenes (**BST[*n*]**) and bridged phenylstilbenes (**BPST[*n*]**). Calculating the non-radiative decay pathway of **BST[*n*]**, we qualitatively predicted the trend of the fluorescence quantum

yields of this series of molecules. The calculated results suggest that **BST[5]** has a high fluorescence quantum yield (Φ_{fl}) and that **BST[7]** has a low Φ_{fl}. We then synthesized the **BST[*n*] (5-7)** and the **BPST[*n*] (5-8)** and compared the experimentally obtained results with the calculated predictions. Different luminescent properties such as aggregation-induced emission (AIE), aggregation-induced emission enhancement (AIEE), and aggregation-caused quenching (ACQ) were observed, depending on the structure of the stilbene. **BPST[7]** showed excellent AIE properties (Φ_{sol} = 0.02; Φ_{solid} = 0.75). Experimental Φ_{fl} were rationalized qualitatively based on the predicted energy difference between the Franck-Condon (FC) state and the minimum energy conical intersection (MECI). We discovered that the length of the alkyl chain serves two important roles: a) mechanical control of the CI, and b) controlling the FC via distortion of the π-conjugation plane. These two effects are synergistic, and thus shorter alkyl chains increase the Φ_{sol}, while longer alkyl chains decrease the Φ_{sol}. The extension of the π-conjugation of the system lowers the FC and the local minimum near the FC (S1min). The balance of these three effects determines the overall photophysical properties of the stilbenes and the bridged stilbenes. Based on the theoretical predictions, we succeeded in designing and synthesizing new AIEgens. We are currently designing new dyes using this strategy and investigating the use of bridged stilbenes in applications such as sensors, liquid crystals, and supramolecular chemistry.

Acknowledgements

I would like to thank Prof. Dr. Katsumi Tokumaru for fruitful discussion. This work is partially supported by the Grant-in-Aid for Scientific Research (B) (18H02045), Innovative Areas “π-System Figuration” (17H05145) and “Soft Crystals” (17H06371), JSPS Fellows (16J10324), JSPS Overseas Research Fellowships, and the Cooperative Research Program “NJRC Mater. & Dev.” from MEXT of Japan. All computational investigations were performed on the computers in Research Center for Computational Science, Okazaki, Japan.

Keywords: aggregation induced emission (AIE) • stilbene • environmental responsive non-radiative decay • control of conical intersection accessibility (CCIA) • potential energy surface (PES)

[1] a) J. Mei, N. L. C. Leung, R. T. K. Kwok, J. W. Y. Lam, B. Z. Tang, *Chem. Rev*. **2015**, *115*, 11718–11940; b) J. Mei, Y. Hong, J. W. Y. Lam, A. Qin, Y. Tang, B. Z. Tang, *Adv. Mater*. **2014**, *26*, 5429–5479; c) D. Ding, K. Li, B. Liu, B. Z. Tang, *Acc. Chem. Res*. **2013**, 46, 2441–2453; d) Y. Chen, J. W. Y. Lam, R. T. K. Kwok, B. Liu, B. Z. Tang, *Mater. Horiz*. **2019**, *6*, 428–433; e) S. Sasaki, G. P. C. Drummen, G. Konishi, *J. Mater. Chem. C* **2016**, *4*, 2731–2742; f) Z. Zhao, H. Zhang, J. W. Y. Lam, B. Z. Tang, *Angew. Chem. Int. Ed*. **2020**, in press; *Angew. Chem*. **2020**, in press. [DOI: 10.1002/anie.201916729]; S. Suzuki, S. Sasaki, A. S. Sairi, R. Iwai, B. Z. Tang, G. Konishi, *Angew. Chem. Int. Ed*. **2020**, in press; *Angew. Chem*. **2020**, in press. [DOI: 10.1002/anie.202000940]

[2] a) R. Hu, N. L. C. Leung, B. Z. Tang, *Chem. Soc. Rev*. **2014**, *43*, 4494-4562; b) G. X. Feng, B. Liu, *Acc. Chem. Res*. **2018**, *51*, 1404-1414; c) J. Qi, C. Chen, D. Ding, B. Z. Tang, *Adv. Healthcare Mater*. **2018**, *7*, 1800477; d) T. Y. Huang, W. Jiang, L. Duan, *J. Mater. Chem*.**2018**, *6*, 5577-5596; e) A. S. Sairi, G. Konishi, *Asian J. Org. Chem*. **2019**, *8*, 404–410; f) S. Sasaki, Y. Sugita, M. Tokita, T. Suenobu, O. Ishitani, G. Konishi, *Macromolecules* **2017**, 50, 3544–3556; g) G. Iasilli, A. Battisti, F. Tantussi, F. Fuso, M. Allegrini, G. Ruggeri, A. Pucci, *Macromol. Chem. Phys*. **2014**, *215*, 499-506; h) L. Xu, L. Xu, Z. Wang, R. Wang, L. Wang, X. He, H. Jiang, H. Tang, D. Cao, B. Z. Tang, *Angew. Chem. Int. Ed*. **2020**, in press; *Angew. Chem*. **2020**, in press. [DOI: 10.1002/anie.201907678]; i) C. Wang, Q. Qiao, W. Chi, J. Chen, W. Liu, D. Tan, S. McKechnie, D. Lyu, X. F. Jiang, W. Zhou, N. Xu, Q. Zhang, Z. Xu, X. Liu, *Angew. Chem. Int. Ed*. **2020**, in press; *Angew. Chem*. **2020**, in press. [DOI: 10.1002/anie.201916357]; k) G. Wang, L. Zhou, P. Zhang, E. Zhao, L. Zhou, D. Chen, J. Sun, X. Gu, W. Yang, B. Z. Tang, *Angew. Chem. Int. Ed*. **2020**, in press; *Angew. Chem*. **2020**, in press. [DOI: 10.1002/anie.201913847].

[3] a) J. S. Wu, M. W. Liu, J. C. Ge, H. Y. Zhang, P. F. Wang, *Chem. Soc. Rev*. **2011**, *40*, 3483-3495; b) J. Q. Dong, X. Li, K. Zhang, Y. D. Yuan, Y. X. Wang, L. Z. Zhai, G. L. Liu, D. Q. Yuan, J. W. Jiang, D. Zhao, *J. Am. Chem. Soc*. **2018**, *140*, 4035-4046; c) Y. H. Cheng, J. G. Wang, Z. J. Qiu, X. Y. Zheng, N. L. C. Leung, J. W. Y. Lam, B. Z. Tang, *Adv. Mater*. **2017**, *29*, 1703900; d) H. Yang, M. Li, C. Li, Q. Luo, M. Q. Zhu, H. Tian, W. H. Zhu, *Angew. Chem. Int. Ed*. **2020**, in press; *Angew. Chem*. **2020**, in press. [DOI: 10.1002/anie.201909830]; e) J. Y. Zeng, X. S. Wang, B. R. Xie, M. J. Li, X. Z. Zhang, *Angew. Chem. Int. Ed*. **2020**, in press; *Angew. Chem*. **2020**, in press. [DOI: 10.1002/anie.201912594].

[4] a) N. Adarsh, A. S. Klymchenko, *Nanoscale* **2019**, *11*, 13977-13987; b) Y. Y. Yuan, C. J. Zhang, M. Gao, R. Y. Zhang, B. Z. Tang, B. Liu, *Angew. Chem. Int. Ed*. **2015**, *54*, 1780-1786; *Angew. Chem*. **2015**, *127*, 1800-1806; c) Z. Zheng, T. F. Zhang, H. X. Liu, Y, C. Chen, R. T. K. Kwok, C. Ma, P. F. Zhang, H. H. Y. Sung, D. Williams, J. W. Y. Lam, K. S. Wong, B. Z. Tang, *ACS Nano* **2018**, *12*, 8145-8159; d) J. Qi, C. W. Sun, A. Zebibula, H. Q. Zhang, R. T. K. Kwok, X. Y. Zhao, W. Xi, J. W. Y. Lam, J. Qian, B. Z. Tang, *Adv. Mater*. **2018**, *30*, 1706856; e) J. Ouyang, L. Sun, Z. Zeng, C. Zeng, F. Zeng, S. Wu, *Angew. Chem. Int. Ed*. **2020**, in press; *Angew. Chem*. **2020**, in press. [DOI: 10.1002/anie.201913149]; f) L. Shi, Y. H. Liu, K. Li, A. Sharma, K. K. Yu, M. S. Ji, L. L. Li, Q. Zhou, H. Zhang, J. S. Kim, X. Q. Yu, *Angew. Chem. Int. Ed*. **2020**, in press; *Angew. Chem*. **2020**, in press. [DOI: 10.1002/anie.201909498].

[5] J. Luo, Z. Xie, J. W. Y. Lam, L. Cheng, H. Chen, C. Qiu, H. S. Kwok, X. Zhan, Y. Liu, D. Zhuc, B. Z. Tang, *Chem. Commun*. **2001**, 1740–1741

[6] H. Tong, Y. Hong, Y. Dong, M. Häußler, J. W. Y. Lam, Z. Li, Z. Guo,. Z. Guoa, B. Z. Tang, *Chem. Commun*. **2006**, 1740–1741.

[7] a) J. Chen, C. C. W. Law, J. W. Y. Lam, Y. Dong, S. M. F. Lo, I. D. Williams, D. Zhu, B. Z. Tang, *Chem. Mater*. **2003**, *15*, 1535–1546; b) N. L. C. Leung, N. Xie, W. Z. Yuan, Y. Liu, Q. Wu, Q. Peng, Q. Miao, J. W. Y. Lam, B. Z. Tang, *Chem. Eur. J*. **2014**, *20*, 15349–15353.

[8] a) R. Crespo-Otero, Q. Li, L. Blancafort, *Chem. Asian J*. **2019**, *14*, 700–714; b) S. Suzuki, S. Maeda, K. Morokuma, *J. Phys. Chem. A* **2015**, *119*, 11479–11487.

[9] S. Sasaki, K. Igawa, G. Konishi, *J. Mater. Chem. C* **2015**, *3*, 5940–5950.

[10] S. Sasaki, S. Suzuki, W. M. C. Sameera, K. Igawa, K. Morokuma, G. Konishi, *J. Am. Chem. Soc*. **2016**, *138*, 8194–8206.

[11] S. Sasaki, S. Suzuki, K. Igawa, G. Konishi, *J. Org. Chem*. **2017**, *82*, 6865–6873.

[12] a) A. L. Sobolewski, W. Domcke, *Chem. Phys*. **2000**, *259*, 181-191; b) W. Domcke, D. R. Yarkony, *Annual Rev. Phys. Chem*. **2012**, *63*, 325-352; c) B. Marchetti, T. N. V. Karsili, M. N. R. Ashfold, W. Domcke, *Phys. Chem. Chem. Phys*. **2016**, *18*, 20007-20027; d) B. F. E. Curchod, T. J. Martínez, *Chem. Rev*. **2018**, *118*, 3305-3336.

[13] a) Schilling C. L.; Hilinski, E. F. *J. Am. Chem. Soc*. **1988**, *110*, 2296; b) Tahara, T.; Hamaguchi, H. *Chem. Phys. Lett*. **1994**, *217*, 369.

[14] K. Kokado, T. Machida, T. Iwasa, T. Taketsugu, K. Sada, *J. Phys. Chem. C* **2017**, *122*, 245–251.

[15] a) H. Tsuji, E. Nakamura, *Acc. Chem. Res*. **2019**, *52*, 2939–2949; b) X. Zhu, H. Tsuji, J. T. López Navarrete, J. Casado, E. Nakamura, *J. Am. Chem. Soc*. **2012**, *134*, 19254–19259.

[16] S. Maeda, K. Ohno, K. Morokuma, *J. Chem. Theory Comput.*, **2010** 6, 1538–1545.

[17] GAMESS, M. W.Shmidt, K. K. Baldridge, J. A. Boatz, S. T. Elbert, M. S. Gordon, J. H. Jensen, S. Koseki, N. Matsunaga, K. A. Nguyen, S. J.

Su, T. L. Windus, M. Dupuis, J. A. Montgomery, *J. Comput. Chem.* **1993**, 14, 1347-1363

[18] Gaussian 16, Revision C.01, M. J. Frisch, G. W. Trucks, H. B. Schlegel, G. E. Scuseria, M. A. Robb, J. R. Cheeseman, G. Scalmani, V. Barone, G. A. Petersson, H. Nakatsuji, X. Li, M. Caricato, A. V. Marenich, J. Bloino, B. G. Janesko, R. Gomperts, B. Mennucci, H. P. Hratchian, J. V. Ortiz, A. F. Izmaylov, J. L. Sonnenberg, D. Williams-Young, F. Ding, F. Lipparini, F. Egidi, J. Goings, B. Peng, A. Petrone, T. Henderson, D. Ranasinghe, V. G. Zakrzewski, J. Gao, N. Rega, G. Zheng, W. Liang, M. Hada, M. Ehara, K. Toyota, R. Fukuda, J. Hasegawa, M. Ishida, T. Nakajima, Y. Honda, O. Kitao, H. Nakai, T. Vreven, K. Throssell, J. A. Montgomery, Jr., J. E. Peralta, F. Ogliaro, M. J. Bearpark, J. J. Heyd, E. N. Brothers, K. N. Kudin, V. N. Staroverov, T. A. Keith, R. Kobayashi, J. Normand, K. Raghavachari, A. P. Rendell, J. C. Burant, S. S. Iyengar, J. Tomasi, M. Cossi, J. M. Millam, M. Klene, C. Adamo, R. Cammi, J. W. Ochterski, R. L. Martin, K. Morokuma, O. Farkas, J. B. Foresman, and D. J. Fox, Gaussian, Inc., Wallingford CT, 2016.

[19] a) N. Miyaura, A. Suzuki, *Chem. Rev*. **1995**, *95*, 2457-2483; b) P. Y. Wong, W. K. Chow, K. H. Chung, C. M. So, C. P. Lau, F. Y. Kwong, *Chem. Commun.,* **2011**, *47*, 8328–8330; c) Z. Huang, Z. Liu, J. Zhou, *J. Am. Chem. Soc.,* **2011**, *133*, 15882–15885; d) H. Kotaka, G. Konishi, K. Mizuno, *Tetrahedron Lett.* **2010**, *51*, 181-184.

[20] J. Tatchena, E. Pollakb, *J. Chem. Phys.* **2008**, *128*, 164303.

[21] J. Gierschner, H. G. Mack, L. Lüer, D. Oelkrug, *J. Chem. Phys*. **2001**, *116*, 8596-8609.

[22] T. Itoh, *J. Chem. Phys.* **2005**, *123*, 064302.

[23] S. R. Amrutha, M. Jayakannan, *J. Phys. Chem. B* **2006**, *110*, 4083-4091.

[24] T. Suenobu, I. Arahori, K. Nakayama, T. Suzuki, R. Katoh, T. Nakagawa, *J. Phys. Chem. A* **2020**, *124*, 1, 46-55.

[25] R. Engleman, J. Jortner, *Mol. Phys*. **1970**, *18*, 145-151.

10.1002/anie.202000943

Entry for the Table of Contents

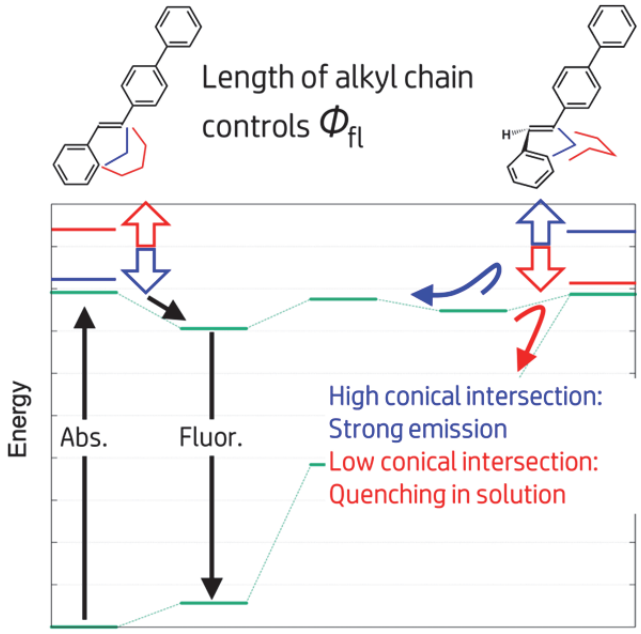

Bridged-stilbene: Based on theoretical prediction of non-radiative decay, a new family of aggregation-induced emission (AIE) luminogens is reported. Depending on alkyl chain length, they exhibit different quantum yields. **BPST[7]** and **DPB[7]** with excellent AIE behavior are reported.